

Performance of Concrete Made with Superplasticizer from Modified Black Liquor and Polycarboxylate

Tailong Zhang,^{a,*} Jianming Gao,^b Bing Qi,^b and Yanling Liu^b

A new kind of retarding polycarboxylate superplasticizer (M20S80) was prepared through the modification of black liquor and polycarboxylate superplasticizer (S) through an Fe^{2+} - H_2O_2 reaction system. The synthesis process of M20S80 was introduced. Infrared spectrum analysis (FT-IR) was used to investigate the changes in functional groups in M20S80. At the same time, a mixture of LM20S80 was made by mixing black liquor and S at a mass ratio of 1:4 directly at room temperature. In comparison with S and LM20S80, the influences of M20S80 on the properties of concrete were studied. The results indicate that M20S80 had a better water reduction rate in concrete than LM20S80 and was close to S under the same conditions. Furthermore, M20S80 had a retarding effect on the early strength development of concrete, but no negative influence on strength after 28 d of curing. Finally, M20S80 with dosages of 0.45% appeared to be more effective in improving the pore structure of concrete.

Keywords: Black liquor; Polycarboxylate superplasticizer; Chemical modification; Concrete; Infrared spectrum analysis

Contact information: a: Jiangsu Key Laboratory of Construction Materials, Southeast University, Nanjing 211189, China; b: Department of Materials Science & Engineering, Southeast University, Nanjing 211189, China; *Corresponding author: zhangtailong1976@163.com

INTRODUCTION

Superplasticizer is an important chemical admixture commonly used in the preparation of concrete (Ouyang *et al.* 2009). These admixtures with comb-branched chains (Lei *et al.* 2013) are adsorbed on cement particles, creating electrostatic repulsions (Chen *et al.* 2012). By overcoming attractive forces (Bonen and Sarkar 1995), such usage of superplasticizers improves the workability of concrete (Hanehara and Yamada 1999). Moreover, they can reduce the water requirements of concrete while maintaining the flow characteristics in a suitable range. As a result, properties of concrete such as comprehensive strength, microstructure, and durability are improved.

Black liquor is a by-product of the papermaking industry (He *et al.* 2014). The total global potential of black liquor is enormous (Huang and Ramaswamy 2011) and most of it serves as fuel, causing high energy waste and serious environmental pollution (Zhang and Tu 2011; Ye *et al.* 2014). To take full advantage of these renewable resources, people began to make lignosulfonate as a concrete admixture from black liquor in the 1930s (Chang and Chan 1995; Nadif *et al.* 2002; Kamoun *et al.* 2003). Because of its structure, with specific functional groups such as $-\text{SO}_3^{2-}$, $-\text{OH}$, and $-\text{O}-$, lignosulfonate has a high level of reactivity (Malutan *et al.* 2008a,b) and has been widely used for producing water-reducing admixtures (Chang and Chan 1995; Yousuf *et al.* 1995; Kamoun *et al.* 2003). However, because of poor water reduction rates and an obvious retarding effect, lignosulfonate cannot completely meet the requirements for the

construction of modern concrete. Therefore, many modification studies have been carried out in order to improve the performance of lignosulfonate (Yu *et al.* 2013). At present, methods of modification include increasing the number of sulphonic groups, increasing the molecular weight, and copolymerizing with other compounds (Ouyang *et al.* 2006; Pei *et al.* 2008; Areskogh *et al.* 2010).

In this study, a mixture of black liquor and polycarboxylate superplasticizer (S) (black liquor:S 1:4 w/w) was modified by an Fe^{2+} - H_2O_2 reaction system to prepare M20S80, which was characterized by Fourier transform infrared (FT-IR) spectroscopy to investigate variations in functional groups. The modification process of black liquor and S was introduced. In comparison with S and the mixture LM20S80 (made by mixing black liquor and S at a mass ratio of 1:4 directly at room temperature), the water-reducing effect of M20S80 and its influences on compressive strength and the pore structure of concrete were studied.

EXPERIMENTAL

Materials

Black liquor and polycarboxylate superplasticizer were supplied by Jiangsu TMS Concrete Admixture Co., Ltd. in Jiangsu province, PR China. Black liquor was obtained from sulfate pulping of wheat stalk. Its lignin and ash content were determined to be 69.3% and 19.5% according to TAPPI T222 and TAPPI T211, respectively, and the rest of the components were degradative carbohydrates. Table 1 presents the uniformity properties of black liquor and S. The molecular structure of S is shown in Fig. 1. Ferrous sulfate and hydrogen peroxide (analytical purity) were purchased from Huadong Chemicals Co., Ltd. in Jiangsu province, PR China. Portland cement PII42.5R was supplied by Nanjing Jiangnan Cement Co., Ltd. in Anhui province, PR China. The chemical compositions and properties of the cement are shown in Table 2.

Table 1. Properties of Black Liquor and Polycarboxylate Superplasticizer

Name	pH Value	Solid-containing Content
Black liquor	12.5	46%
Polycarboxylate superplasticizer	4.0	40%

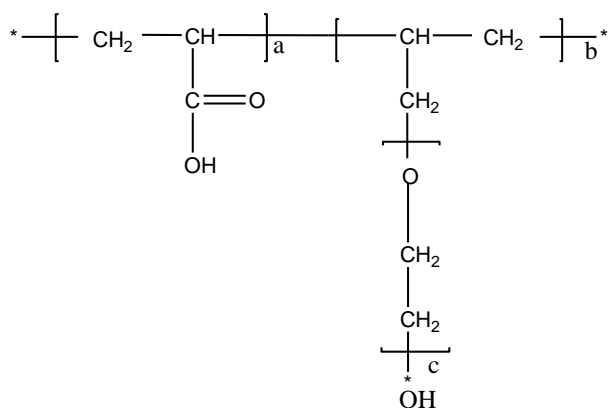


Fig. 1. Molecular structure of the polycarboxylic acid water-reducing agent

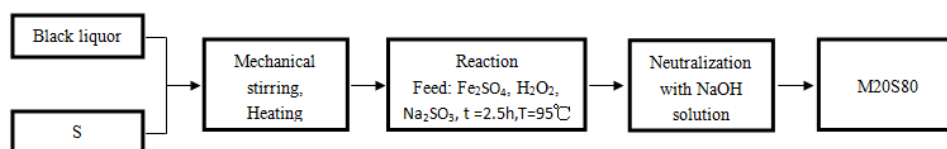
Table 2. Chemical Composition and Physical Properties of Cement

Specific Surface Area (m ² /kg)	Chemical Composition (%)			Normal Consistency (%)	Setting Time (min)	Stability	Flexural Strength (MPa)	Compression Strength (MPa)
	SiO ₂	Al ₂ O ₃	CaO		Initial		3 d	3 d
370	MgO	SO ₃	Fe ₂ O ₃	29	Final	Qualified	28 d	28 d
	Loss				140		5.5	27.5
	20.6	5.03	65.06		195		8.5	55.0
	0.55	2.24	4.38					
		1.30						

Methods

Synthesis process

First, 20 g of black liquor and 80 g of S were placed in a reaction vessel equipped with stirrer, thermometer, and condenser. When the solution was stirred (stirring velocity of 150 r/min) and heated to the reaction temperature, 0.05 g of ferrous sulfate, 0.35 g of hydrogen peroxide, and 4 g of sodium sulfite dissolved in deionized water were added at a constant velocity under stirring to start the reaction, which was carried out at 95 °C for 2.5 h. The pH value was adjusted by adding 35 wt.% NaOH aqueous solution. The reaction mixture was then allowed to cool to room temperature. Finally, the modified M20S80 was obtained with a solid content of 32.26% and a pH value between 8 and 9. The synthesis flow chart of M20S80 is illustrated in Fig. 2. Meanwhile, for comparative study, LM20S80 was also prepared by mixing 20 g of black liquor and 80 g of S directly at room temperature. The pH value of LM20S80 was adjusted to be the same as that of M20S80.

**Fig. 2.** Modification scheme of black liquor and S

Concrete specimens

According to the proportions, the materials were weighed, and the cement, coarse aggregates, and fine aggregates were mixed in dry state. After adding water, with or without concrete admixture, all materials were mixed together to obtain a homogeneous mixture and cast in steel molds 150 mm x 150 mm x 150 mm. The concrete was removed from the molds 24 h after casting, and cured at 20 ± 3 °C and 95% of relative humidity. The concrete made without concrete admixture was defined as K, which was used as a reference sample.

Water-reducing rate (WR)

The water-reducing rate was tested according to the Chinese standard GB/T 8076 (2008), which was determined using Eq. 1,

$$W_R = (W_0 - W_1) / W_0 * 100\%, \quad (1)$$

where W_0 is the water consumption of the reference concrete and W_1 is the water consumption of the test concrete made with concrete admixtures.

Fourier transform infrared spectroscopy (FT-IR)

Fourier transform infrared spectroscopy was performed with a Bio-Rad FTS 6000 FTIR (USA) using KBr pellet techniques to measure the energy absorption of the ancient samples. Here, 3 mg of finely-ground (< 80- μ m) specimen powder was homogeneously ground with 300 mg of KBr powder until the mixture had the consistency of fine flour, and was then pressed into a thin 15-mm-diameter disc.

Compressive strength

The compressive strengths of the specimens cured for 3, 7, and 28 days were measured using a closed-loop servo-hydraulically-controlled materials testing machine (MTS 810, USA) following the ASTM C270-12a (2012) standard. The stress was regularly increased at a rate of 0.02 MPa/sec and the peak value attained when the cube ruptured, and was recorded as the uniaxial compressive strength (q_{dry}). At least three specimens were tested for each formula mix, and the average value was defined as the ultimate strength.

Mercury intrusion porosimetry (MIP)

The porosity and pore size distribution of concrete at different ages were determined using a mercury intrusion porosimeter (AutoPore IV 9500; Micromeritics, USA) capable of generating pressure in the range of subambient to 33000 psi. The pore radius calculation was done using the Washburn's equation (Kumar and Bhattacharjee 2003), *i.e.*, $r = -2 * \gamma * \cos\theta / P$, where r is the pore entry radius in which mercury is being intruded, γ is surface tension, and θ and P are the contact angles of mercury with solid and applied pressure, respectively.

RESULTS AND DISCUSSION

FT-IR Characterization

The infrared spectrum is often used to give information about the composition of a sample and its structure. Figures 3 and 4 represent the infrared spectrum of LM20S80 and M20S80, respectively. As shown in Fig. 3, the main specific absorption peaks of LM20S80 appeared at 3404.60 cm^{-1} , 1602.06 cm^{-1} , 1433.43 cm^{-1} , 1176.17 cm^{-1} , and 1047.11 cm^{-1} , which were assigned to the O-H stretching vibration, the C=O stretching vibration in the carboxyl group, the C=C stretching vibration in the benzene, the SO₂ symmetrical stretching vibration in the sulfonic group, and the -SO₃ stretching vibration, respectively. As shown in Fig. 4, the main specific absorption peaks of modified M20S80 were observed at about 3408.04 cm^{-1} , 2879.76 cm^{-1} , 1571.95 cm^{-1} , 1343.95 cm^{-1} , 1106.47 cm^{-1} , 937.84 cm^{-1} , and 885.35 cm^{-1} , and were attributed to the O-H stretching vibration, the CH₂ symmetrical stretching vibration, the C=O stretching vibration, the SO₂ anti-symmetrical stretching vibration in the sulfonic group, the C-O-C stretching vibration, the COH out-of-plane bending vibration, and the S-O stretching vibration, respectively. The above analysis showed that the absorption peaks of carboxyl

group and C-O-C were more apparent after modification. This was probably a consequence of oxidation, which converted carbonyl, hydroxyl group, and phenolic hydroxyl groups in lignin to carboxyl groups. It was implied that, meanwhile, graft reaction between lignin and S occurred through free radical polymerization.

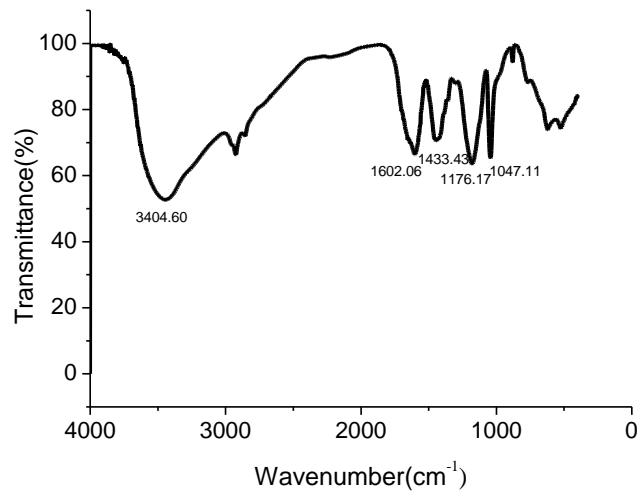


Fig. 3. Infrared spectrum of LM20S80

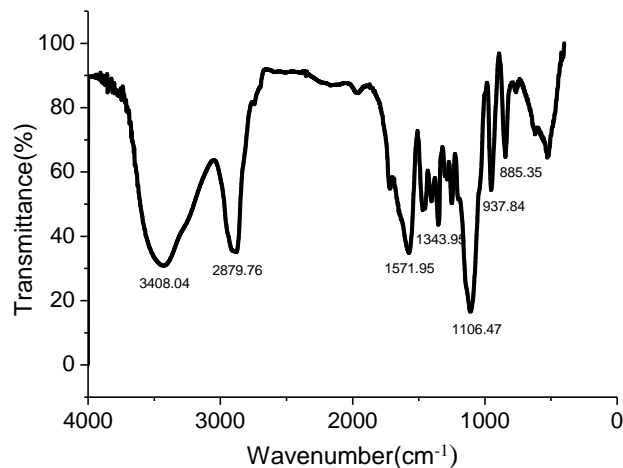


Fig. 4. Infrared spectrum of M20S80

Water-reducing Rate

Figure 5 shows the water-reducing rate of concrete with different dosages of M20S80. The water-reducing rate of concrete was 16.8% when 0.35 wt.% of M20S80 was used. With increasing M20S80 dosages, the water-reducing rate of concrete increased. For example, when the M20S80 dosages increased from 0.35% to 0.45%, the water-reducing rate of concrete increased from 16.8% to 27.6%. However, when the M20S80 dosages continued to increase, the growth rate of the water-reducing rate started falling. These results indicate that there must be an optimal M20S80 dosage. When the optimal dosage was exceeded, the growth rate of the water-reducing rate of concrete with M20S80 was limited.

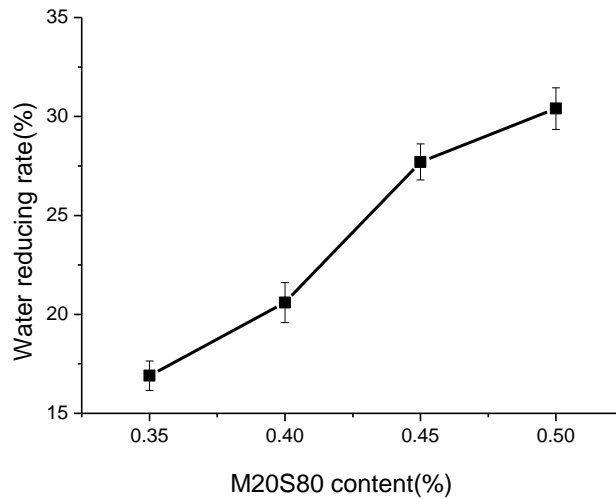


Fig. 5. Effect of M20S80 dosage on the water-reducing rate of concrete

Figure 6 shows variations in the water-reducing rates of S, LM20S80, and M20S80 with the same dosage of 0.45%. The water-reducing rate of concrete with S, LM20S80, and M20S80 was 30.8%, 25.8%, and 30.3%, respectively. This means that the water-reducing rate of M20S80 was obviously better than that of LM20S80, but slightly worse than that of S. The results indicate that chemical modification effectively improved the water-reducing rate of M20S80, which was comparable to that of the pure polycarboxylate superplasticizer.

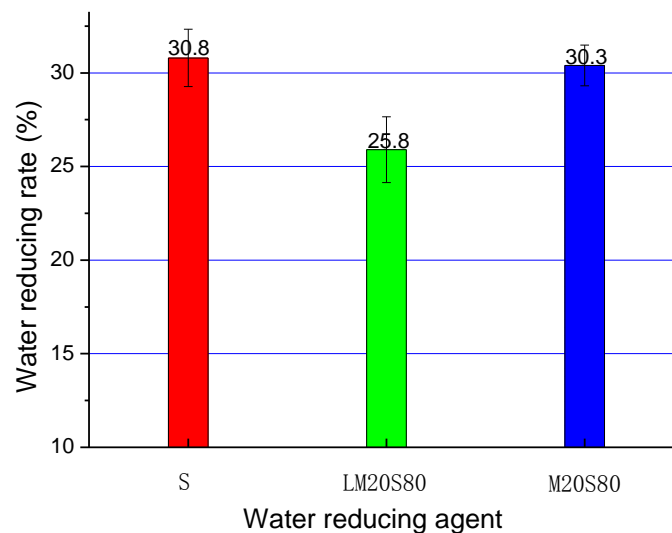


Fig. 6. Variations in the water-reducing rate of concrete with different water-reducing agents

Compressive Strength

Figure 7 presents the influence of M20S80 dosages on the compressive strength of concrete. As shown in Fig. 7, with increasing M20S80 content, the compressive strength of concrete increased accordingly after 3, 7, and 28 days. This can be interpreted

to mean that M20S80 promotes the better dispersion of cement paste, which is beneficial to cement hydration and the development of the concrete's pore structure. With the thorough interspersing and overlapping of cement hydration products, the structure of concrete became much denser. Therefore, the compressive strength of concrete increased gradually.

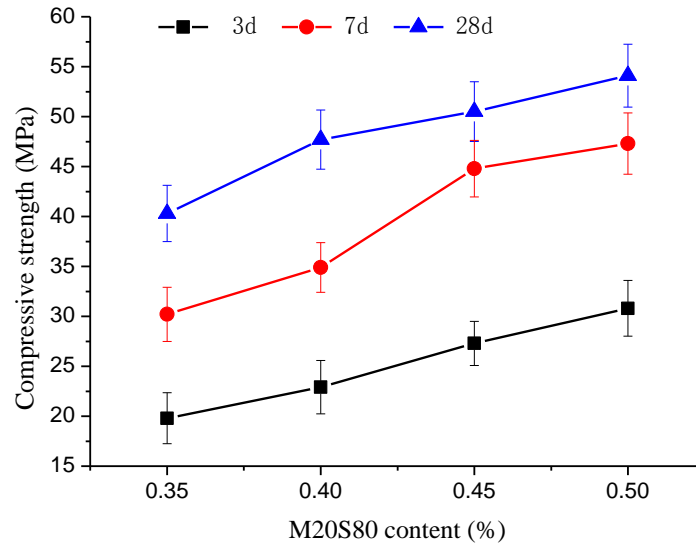


Fig. 7. Effect of M20S80 dosages on the compressive strength of concrete

Figure 8 shows variations in the compressive strength of concrete cured for 3, 7, and 28 days. Compared with the reference sample (K), the compressive strength of concrete with the same dosages of S, LM20S80, and M20S80 were obtained. According to the results, the compressive strength of concrete with the water-reducing agent was higher than that of the blank concrete at every curing age.

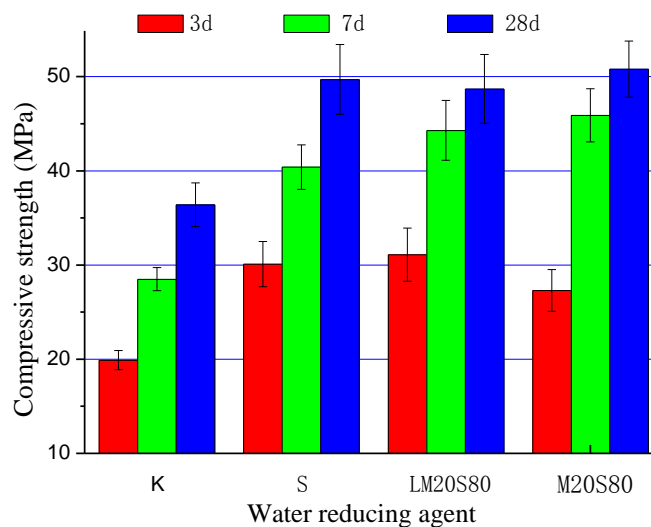


Fig. 8. Variations in the compressive strength of concrete with different water-reducing agents

It can be seen in Table 3 that the compressive strength ratios of concrete with S, LM20S80, and M20S80 were 151%, 156%, and 137%, respectively, after curing for 3 days. This revealed that M20S80 delayed the initial hydration of cement in comparison with S and LM20S80. However, according to the results for 28 days of curing, the compressive strength ratios of concrete with S, LM20S80, and M20S80 were 137%, 134%, and 139%, respectively. The M20S80 had no adverse effect on the long-term strength of concrete. From the above results, it is believed that M20S80 was a kind of retarded type high-range superplasticizer.

Pore Structure of Concrete

Table 3 shows variations in the pore structure of concrete with different water-reducing agents. The most probable pore sizes of concrete with the same contents of S, LM20S80, and M20S80 were 38.33 nm, 55.54 nm, and 47.03 nm, respectively, while the most probable pore size of blank concrete (K) was 77.25 nm, which was shown in Fig. 9. The pore structure of concrete was improved when the water-reducing agent was used. According to the total porosity results in Table 3, the concrete with M20S80 had the smallest total porosity with the same water-reducing agent content. In addition, with the increase of M20S80 dosages from 0.35% to 0.50%, the total porosity of concrete decreased from 15.87% to 13.43%, and the most probable pore size of concrete decreased from 69.12 nm to 40.33 nm, as shown in Fig. 10. These results imply that M20S80 performed better for improving the pore structure of concrete. This may be attributed to the fact that M20S80 improved the dispersion of cement and the growth of hydration products because of its excellent water-reducing ability and certain retarding propensity.

Table 3. Influence of Water-reducing Agent on Pore Size Distribution

	Content	Pore Size Distribution (%)				Void Volume (10 ⁻⁴ mL/g)	Total Porosity (%)
		0 to 20 (nm)	20 to 100 (nm)	100 to 200 (nm)	>200 (nm)		
K	-	24.40	25.91	8.93	40.76	850.95	17.24
S	0.45%	34.32	35.45	5.16	25.07	544.21	14.40
LM20S80	0.45%	32.15	30.55	7.94	29.36	653.02	14.80
M20S80	0.35%	33.91	27.34	8.72	30.03	594.85	15.87
	0.40%	36.73	29.83	4.92	28.52	557.98	14.92
	0.45%	33.66	35.07	9.74	21.53	543.98	14.39
	0.50%	30.65	35.91	6.31	27.13	530.09	13.43

K, blank concrete; S, polycarboxylate superplasticizer

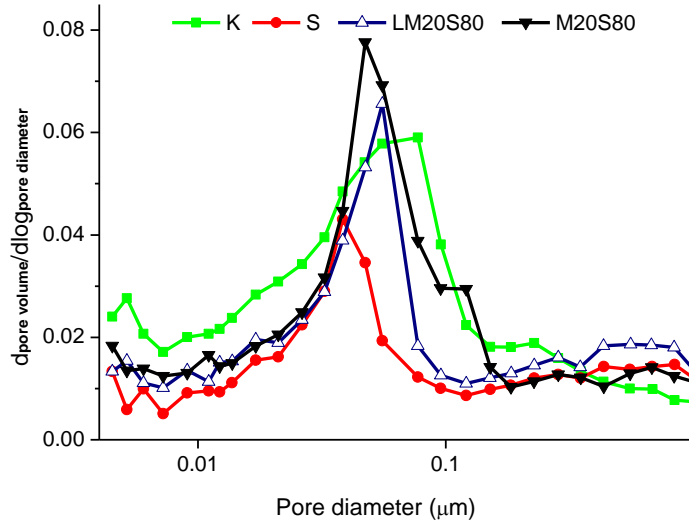


Fig. 9. Effect of water-reducing agent amount on pore size distribution of concrete

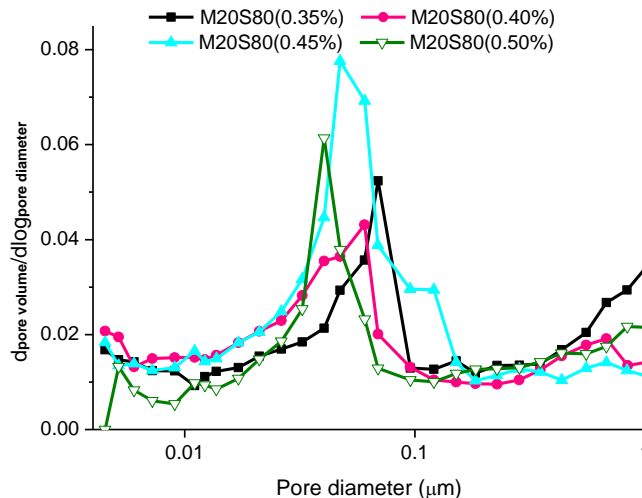


Fig. 10. Effect of M20S80 dosage on pore size distribution of concrete

CONCLUSIONS

From the above testing results and discussion, the modification process was judged to be successful, such that 20 wt.% of S could be replaced by black liquor, which would produce enormous economic benefits. In the future, a production-scale trial will be carried out as a step in the transfer of technology.

1. The results of infrared spectra analysis showed that after chemical modification with an Fe^{2+} - H_2O_2 reaction system, M20S80 had a different molecular structure. The product obtained was a new type of water-reducing agent, which had better water-reducing ability than LM20S80 and was comparable to the pure polycarboxylate superplasticizer.

2. The M20S80 acted as a kind of retarded water-reducing agent. Compared with concrete treated with S and LM20S80, the concrete treated with M20S80 after curing for 3 d had lower compressive strength. However, M20S80 had no negative effect on the long-term strength of concrete.
3. Because of chemical modification, M20S80 showed good performance in water-reducing and retarding effects. Compared with LM20S80 and S, concrete mixed with M20S80 had better pore size distribution and smaller total porosity.

REFERENCES CITED

- ASTM C270.12a. (2012). "Standard specification for mortar for unit masonry," ASTM International West Conshohocken, PA.
- Areskog, D., Li, J. B., Gellerstedt, G., and Henriksson, G. (2010). "Investigation of the molecular weight increase of commercial lignosulfonates by laccase catalysis," *Biomacromolecules* 11(4), 904-910. DOI: 10.1021/bm901258v
- Bonen, D., and Sarkar, S. L. (1995). "The superplasticizer adsorption capacity of cement pastes, pore solution composition, and parameters affecting flow loss," *Cem. Concr. Res.* 25(5), 1423-1434. DOI: 10.1016/0008-8846(95)00137-2
- Chang, D. Y., and Chan, S. Y. N. (1995). "Straw pulp waste liquor as a water-reducing admixture," *Cem. Concr. Res.* 47(171), 113-118. DOI: 10.1680/mac.1995.47.171.113
- Chen, W., Shen, P., Shui, Z., and Fan, J. (2012). "Adsorption of superplasticizers in fly ash blended cement pastes and its rheological effects," *J. Wuhan Univ. Technol. Mater.* 27(4), 773-778. DOI: 10.1007/s11595-012-0546-8
- GB/T 8076. (2008). *Concrete Admixtures*, Chinese National Standardization Management Committee, China.
- Hanehara, S., and Yamada, K. (1999). "Interaction between cement and chemical admixture from the point of cement hydration, absorption behaviour of admixture, and paste rheology," *Cem. Concr. Res.* 29(8), 1159-1165. DOI: 10.1016/S0008-8846(99)00004-6
- He, L., Liu, Q., Song, Y., and Deng, Y. (2014). "Effect of metal chlorides on the solubility of lignin in the black liquor of prehydrolysis kraft pulping," *BioResources* 9(3), 4636-4642.
- Huang, H., and Ramaswamy, S. (2011). "Thermodynamic analysis of black liquor steam gasification," *BioResources* 6(3), 3210-3230.
- Kamoun, A., Jelidi, A., and Chaabouni, M. (2003). "Evaluation of the performance of sulfonated esparto grass lignin as a plasticizer water reducer for cement," *Cem. Concr. Res.* 33(7), 995-1003. DOI: 10.1016/S0008-8846(02)01098-0
- Kumar, R., and Bhattacharjee, B. (2003). "Porosity, pore size distribution and in situ strength of concrete," *Cem. Concr. Res.* 33(1), 155-164. DOI: 10.1016/S0008-8846(02)00942-0
- Lei, J., Li, H., and Du, X. (2013). "Effect of diester in esterification product of polyethylene glycol and acrylic acid on the performance of polycarboxylate superplasticizer," *Iran. Polym. J.* 22(1), 117-122. DOI: 10.1007/s13726-012-0110-6
- Malutan, T., Nicu, R., and Popa, V. I. (2008a). "Contribution to the study of hydroxymethylation reaction of alkali lignin," *BioResources* 3(1), 13-20.

- Malutan, T., Nicu, R., and Popa, V. I. (2008b). "Lignin modification by epoxidation," *BioResources* 3(4), 1371-1376.
- Nadif, A., Hunkeler, D., and Käuper, P. (2002). "Sulfur-free lignins from alkaline pulping tested in mortar for use as mortar additives," *Bioresour. Technol.* 84(8), 49-55. DOI: 10.1016/S0960-8524(02)00020-2
- Ouyang, X. P., Jiang, X. Y., Qiu, X. Q., Yang, D. J., and Pang, Y. X. (2009). "Effect of molecular weight of sulfanilic acid-phenol-formaldehyde condensate on the properties of cementitious system," *Cem. Concr. Res.* 39(1), 283-288. DOI: 10.1016/j.cemconres.2009.01.002
- Ouyang, X. P., Qiu, X. Q., and Chen, P. (2006). "Physicochemical characterization of calcium lignosulfonate – A potentially useful water reducer," *Colloids Surf. A* 282(20), 489-497. DOI: 10.1016/j.colsurfa.2005.12.020
- Pei, M. S., Li, C., Wang, Z. F., Zhang, J., Qin, X. J., and Liu, L. J. (2008). "The synthesis of carboxyl calcium lignosulfonate and its applications as water reducer," *Dispersion Sci. Technol.* 29(4), 530-534. DOI: 10.1080/01932690701716143
- Ye, D. Z., Jiang, L., Ma, C., Zhang, M. H., and Zhang, X. (2014). "The graft polymers from different species of lignin and acrylic acid: Synthesis and mechanism study," *Int. J. Biol. Macromol.* 63, 43-48. DOI: 10.1016/j.ijbiomac.2013.09.024
- Yousuf, M., Mollah, A., Palta, P., Hess, T. R., Vempati, R. K., and Cocke, D. L. (1995). "Chemical and physical effects of sodium lignosulfonate superplasticizer on the hydration of Portland cement and solidification/stabilization consequences," *Cem. Concr. Res.* 25(3), 671-682. DOI: 10.1016/0008-8846(95)00055-H
- Yu, G., Li, B., Wang, H., Liu, C., and Mu, X. (2013). "Preparation of concrete superplasticizer by oxidation-sulfomethylation of sodium lignosulfonate," *BioResources* 8(1), 1055-1063.
- Zhang, X., and Tu, M. (2011). "Routes to potential bioproducts from lignocellulosic biomass lignin and hemicelluloses" *BioEnergy Res.* 4(4), 246-257. DOI: 10.1007/s12155-011-9147-1

Article submitted: July 11, 2014; Peer review completed: September 14, 2014; Revised version received and accepted: October 5, 2014; Published: October 23, 2014.